ICES Journal of Marine Science, 2023, **0**, 1–16
DOI: 10.1093/icesjms/fsad070
Original Article

Growth and diet of a larval myctophid across distinct upwelling regimes in the California Current

K. Swieca [1,2,*], S. Sponaugle [1,2], M. S. Schmid [2], J. Ivory[2], M. Corrales-Ugalde [3,4], K. R. Sutherland [3], and R. K. Cowen[2]

[1]Department of Integrative Biology, Oregon State University, Corvallis, Oregon 97331, USA
[2]Hatfield Marine Science Center, Oregon State University, Newport, Oregon 97365, USA
[3]Biology Department, University of Oregon, Eugene, Oregon 97403, USA
[4]Atmospheric and Oceanic Sciences, Princeton University, Princeton, New Jersey 08540, USA

[*] *Corresponding author. tel: (541) 867-0100*; e-mail: swiecak@oregonstate.edu.

Eastern boundary systems support major fisheries of species whose early stages depend on upwelling production. However, upwelling can be highly variable at the regional scale, leading to complex patterns of feeding, growth, and survival for taxa that are broadly distributed in space and time. The northern California Current (NCC) is characterized by latitudinal variability in the seasonality and intensity of coastal upwelling. We examined the diet and larval growth of a dominant myctophid (*Stenobrachius leucopsarus*) in the context of their prey and predators in distinct NCC upwelling regimes. Larvae exhibited significant differences in diet and growth, with greater seasonal than latitudinal variability. In winter, during reduced upwelling, growth was substantially slower, guts less full, and diets dominated by copepod nauplii. During summer upwelling, faster-growing larvae had guts that were more full from feeding on calanoid copepods and relying less heavily on lower trophic level prey. Yet, our findings revealed a dome-shaped relationship with the fastest growth occurring at moderate upwelling intensity. High zooplanktivorous predation pressure led to above average growth, which may indicate the selective loss of slower-growing larvae. Our results suggest that species whose spatio-temporal distributions encompass multiple regional upwelling regimes experience unique feeding and predation environments throughout their range with implications for larval survivorship.

Keywords: fine-scale imaging, larval fish, myctophids, trophic interactions, upwelling.

Introduction

The early life history stages of marine fishes are generally considered a bottleneck for year-class strength and fishery production (Anderson, 1988; Houde, 2008). Survival through these critical periods is largely determined by the ability of larvae to find food and avoid predation in the highly dynamic pelagic environment (Lasker, 1978; Bailey and Houde, 1989). One key physical mechanism that may influence trophic interactions and the subsequent growth, survival, and recruitment (entry into the adult population) of the early life history stages of fishes is upwelling. Coastal upwelling can influence the survival of the early life history stages of fishes directly, by dictating the amount of food available in the water column and, indirectly, by affecting the spatial distributions and encounter rates between larvae, their prey, and their potential predators.

Coastal upwelling is often considered a hallmark for increased food availability, as it promotes enhanced biological productivity (Checkley and Barth, 2009 and references therein). For pelagic larval fishes, high prey availability can lead to high feeding success, fast growth, and large size-at-age of larvae (Pepin *et al.*, 2015). Typically, these traits are thought to increase survival through the vulnerable early life history stages and positively affect year-class strength (Anderson, 1988; Miller *et al.*, 1988; Hare and Cowen, 1997). However, larvae feed selectively on available prey fields and the degree to which increased production confers increasing feeding is unclear (Robert *et al.*, 2014). Further, in addition to increasing potential food availability, coastal upwelling leads to turbulent mixing of the nutrient-rich upper water column and offshore transport of the surface layer. Both processes have the potential to indirectly affect larval survival by modifying larva-prey and larva-predator encounter rates (Lasker, 1978, 1981; Parrish *et al.*, 1981; Gadomski and Boehlert, 1984).

The effect of upwelling on the early life history stages of fishes is highly variable and appears to be system, scale, and taxon dependent. Foundational hypotheses in the field of fisheries oceanography suggest that upwelling may be necessary to replenish surface nutrients, but too much upwelling can disrupt larval food aggregations and/or advect larvae into more oligotrophic conditions offshore ("Stable Ocean Hypothesis"; Lasker, 1978, 1981 and "Optimal Environmental Window"; Cury and Roy, 1989). Hence, there may be a dome-shaped relationship between upwelling intensity and recruitment with the highest survivorship occurring during moderate upwelling conditions when foraging success is high (due to nutrient inputs from upwelled waters coupled with moderate turbulence-induced increased encounter rates) and advection losses are low. Upwelling phenology may also be an important characteristic impacting larval survival, especially in seasonal upwelling systems. For example, in the northern California Current (NCC), a delayed onset of the upwelling season (i.e. the spring transition) resulted in slower growth of northern anchovy (*Engraulis mordax*) larvae, with implication for recruitment (Takahashi *et al.*, 2012). In the NCC, the onset and length of the upwelling season is linked to the arrival and maintenance of a lipid-rich copepod community, which serves

Received: 7 January 2023; **Revised:** 24 March 2023; **Accepted:** 30 March 2023

as important prey base for this species (Hooff and Peterson, 2006).

Variability in upwelling characteristics (i.e. intensity, duration, and phenology) leads to complex patterns of feeding, growth, and survival of young fish. Yet, studies of variability in larval and juvenile growth and feeding across different upwelling regimes are rare. It is also challenging to simultaneously incorporate the influence of predation on survival due to sampling constraints of net-based systems (i.e. for gelatinous predators). Nonetheless, feeding opportunities are often spatially correlated to predation risk (Bakun, 2006; McClatchie *et al.*, 2012) and predation may be the primary agent of larval mortality (Bailey and Houde, 1989). Here, we analyze larval growth and feeding patterns of a common yet understudied fish relative to prey availability and co-occurring predation pressure in four distinct NCC upwelling regimes.

The NCC is characterized by strong latitudinal gradients in the intensity and seasonality of coastal upwelling. While the central coast of Oregon has distinct downwelling (winter) and upwelling (summer) seasons, northern California typically experiences stronger and more persistent upwelling with more interannual variability. In both locations, occasional winter storms cause deep mixing of the water column and strong turbulence in the surface layer (Bograd *et al.*, 2009; Checkley and Barth, 2009; García-Reyes and Largier, 2012). In the NCC, upwelling is frequently associated with high production and offshore transport of surface waters, while downwelling leads to decreased production, reduced water column stratification, and onshore transport (Checkley and Barth, 2009). Variability in regional upwelling leads to changes in the community structure of zoo- and ichthyoplankton (Hooff and Peterson, 2006; Auth, 2008), with implications for species interactions and survival of young fishes.

Widely distributed from northern Baja California (~30°N) to the Bering Sea (~55°N; Matarese *et al.*, 1989; Beamish *et al.*, 1999; Brodeur and Yamamura, 2005), the northern lampfish (*Stenobrachius leucopsarus*, Myctophidae) is frequently one of the most abundant larval fish in the California Current (e.g. Richardson and Pearcy, 1977; Auth and Brodeur, 2006; McClatchie *et al.*, 2018). They are small-bodied as adults, short-lived, and can be considered a forage fish. Mature northern lampfish have a protracted spawning season throughout their range, which typically peaks in March each year (Fast, 1960; Smoker and Pearcy, 1970). Although an early study suggested that their spawning season is shorter off Oregon (October—March; Smoker and Pearcy, 1970), larval northern lampfish are found in high abundances in spring and late summer sampling (April/May—September/October; Richardson and Pearcy, 1977; Auth and Brodeur, 2006) indicating that Oregon spawning encompasses both winter and summer seasons. Northern lampfish eggs are infrequently sampled due to a delicate chorion, so exact size-at-hatch is unknown, but flexion and metamorphosis occur at ~6.5 and 18 mm standard length (SL), respectively (Fast, 1960; Smoker and Pearcy, 1970; Matarese *et al.*, 1989).

Latitudinal variability in the intensity and phenology of upwelling within the range of northern lampfish make this system and species ideal to tease apart relationships between upwelling, trophic interactions, growth, and subsequent survival of young fish. Myctophids represent an important trophic link between zooplankton (e.g. copepods and euphausiids) and large marine predators (e.g. tuna, salmon, seabirds, and marine mammals; Brodeur and Yamamura, 2005). Despite this critical trophic role, northern lampfish are the focus of relatively few studies. Knowledge of their larval stage is particularly scant, with only one study examining larval growth (last 3d growth; Methot, 1981).

We hypothesize that variability in the growth and diet of larval northern lampfish is related to the degree of upwelling and its influence on prey availability and potential predation pressure. To test this, we coupled otolith-derived measures of growth, gut content analysis, and *in situ* plankton imagery in four distinct NCC upwelling regimes: Oregon winter (typically downwelling), Oregon summer (typically moderate upwelling), northern California winter (typically upwelling), and northern California summer (typically strong upwelling). We expected growth to vary seasonally and latitudinally, with higher growth occurring during summer upwelling conditions, especially in moderate Oregon upwelling compared to the more intense upwelling off of northern California.

Materials and methods

Field sampling

Biological net samples and *in situ* plankton imagery were collected during four research cruises in the NCC over a period of two years, with two seasonal cruises in 2018 and two replicate cruises in 2019: winter 2018 (W18; 15–23 February), summer 2018 (S18; 3–11 July), winter 2019 (W19; 3–11 March), and summer 2019 (S19; 16–25 July).

During each cruise, we deployed nets at five stations and continuously towed the plankton imager along two historically sampled cross-shelf transects, the Newport Hydrographic Line (NH; seasonal upwelling) and the Trinidad Head Line (TR; continuous upwelling; Figure 1). Station locations were selected to capture shelf, shelf-break, and offshore environments on each transect. All sampling occurred during full daylight hours.

Biological sample collection

Biological samples were collected with a coupled Multiple Opening/Closing Net and Environmental Sensing System (MOCNESS; Guigand *et al.*, 2005) that simultaneously sampled with five sets of paired nets: 4-m^2 nets fit with 1-mm mesh and 1-m^2 nets fit with 333-μm mesh. The first set of nets were towed obliquely from the surface to depth (max 100-m) and the remaining four sets were triggered remotely to sample discrete 25-m depth bins. This system was towed behind the ship at 0.75-1 m s^{-1} and was fit with a flowmeter and conductivity, temperature, and depth sensors. Replicate MOCNESS tows were performed at every station, except for the W18 cruise, when sampling was limited by winter storm conditions. In addition to MOCNESS sampling, to sample prey that might be excluded from the MOCNESS nets, a 0.2-m^2 vertical ring-net fit with 100-μm mesh and a flowmeter were deployed to 25-m depth at every other station.

Immediately after MOCNESS and ring-net retrieval, nets were rinsed with seawater, sieved, and individually preserved in 95% ethanol. Ethanol was changed within 48 h of collection and again within 2 months to properly preserve otoliths for growth analysis. Fish larvae collected by MOCNESS were sorted in the laboratory, enumerated, and identified to the lowest possible taxonomic level. Northern lampfish were placed in individual vials for future growth and diet analyses. Ring-net samples were processed following Postel *et al.* (2000), with

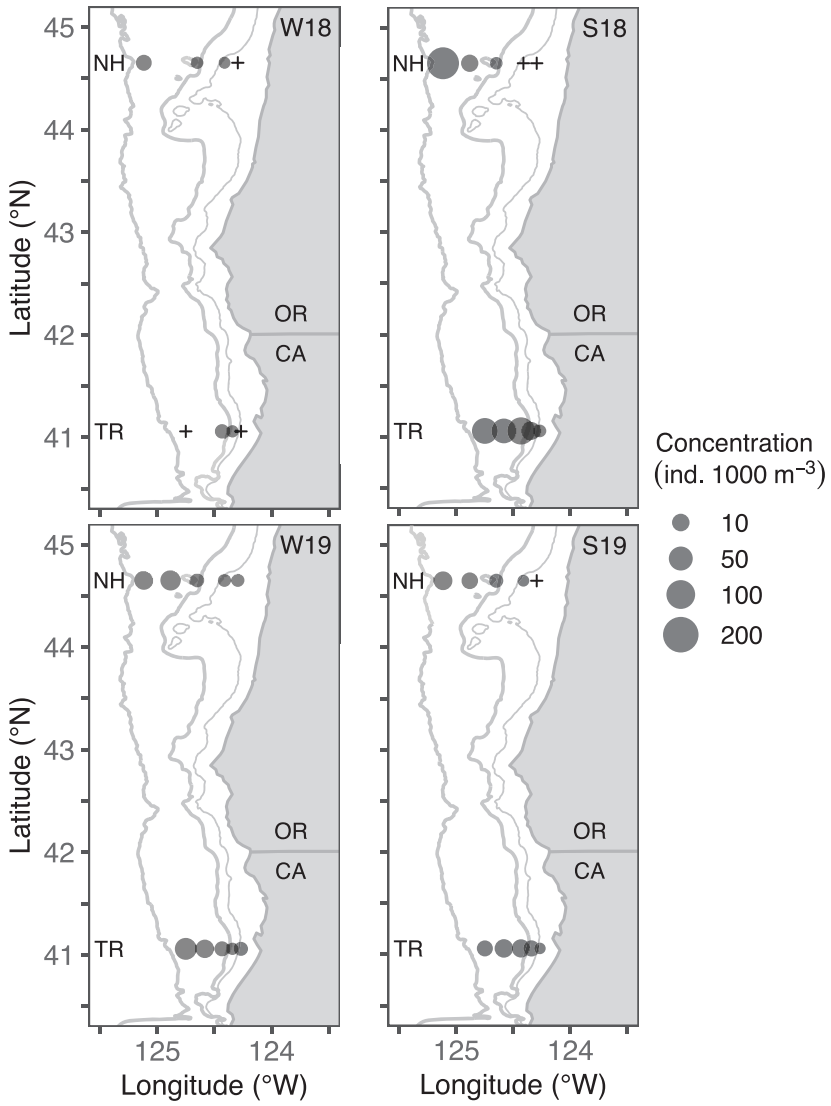

Figure 1. Mean concentration of northern lampfish (*S. leucopsarus*) larvae (individuals 1000 m^{-3}) sampled along the NH Line off the coast of Oregon (OR) and the TR Line off the coast of California (CA) in winter 2018 (W18; 15–23 February), summer 2018 (S18; 3–11 July), winter 2019 (W19; 3–11 March), and summer 2019 (S19; 16–25 July). "+" denotes true zeros and contour lines represent the 100-, 200-, and 2000-m isobaths.

subsamples of 1-5 mL and >200 individuals taken with a Stempel pipette. Zooplankton were enumerated and identified to the lowest possible taxonomic level. Taxa concentrations were calculated for MOCNESS northern lampfish (ind. 1000 m^{-3}) and ring-net zooplankton (ind. m^{-3}) by dividing biological counts from each net by the volume of water filtered through the net.

Imagery data collection

Zooplankton imagery data were collected using the *In situ* Ichthyoplankton Imaging System (ISIIS; Cowen and Guigand, 2008), which was continuously towed the length of each transect within 24 h of every biological sample collection. This resulted in replicate ISIIS tows being performed to align with replicate MOCNESS tows, except for the S18 cruise when a replicate ISIIS tow on the NH Line was not possible. ISIIS is a low turbulence, high-resolution *in situ* shadowgraph imaging system with a large sample volume (150–180 L s^{-1}) and a pixel resolution of 68-μm. Its large field of view (13 × 13 × 50 cm) allows it to capture fragile gelatinous taxa that can be important predators of larval fishes but are difficult to quantify with traditional net-based sampling techniques (McClatchie *et al.*, 2012; Luo *et al.*, 2018). ISIIS was towed at a speed of 2.5 m s^{-1} in a tight undulating fashion from the surface to 100-m depth or within 2.5-m of the seafloor. It was fit with multiple sensors to simultaneously collect physical data including CTD (Sea-Bird SBE49 FastCAT), dissolved oxygen (Sea-Bird 43), fluorescence (Wetlabs FLRT), and photosynthetically active radiation (EPAR; Biospherical QCP-2300). ISIIS data were transferred to ship-board computers via a fiber optic cable.

Growth analysis

We used otolith microstructure analysis to investigate the age and daily growth patterns of larval northern lampfish. Daily otolith increment deposition has been validated for two similar myctophids in the region (*Diaphus theta* and *Tarletonbenia crenularis*: Moku *et al.*, 2001; Bystydzieńska *et al.*, 2010, respectively).

To reduce any variability associated with depth and because we had sufficiently large sample sizes during most cruises, we restricted our growth analyses to MOCNESS larvae collected in the top 50-m of the water column. A random subset of those larvae ($n = 2620$) were measured for SL and body depth to the nearest 0.01-mm using a Leica MZ16 dissecting microscope with a QImaging camera and Image Pro Premier 9.1 software. Random subsamples of ~30 individual northern lampfish were selected from the NH and TR Lines on each cruise for otolith microstructure analysis, except for winter 2018 TR where larvae were damaged due to conditions at sea and all larvae with intact otoliths were used ($n = 6$; total $n = 216$). Larvae <5 mm SL were excluded from otolith analysis (Supplementary Figure S1).

Sagittal otoliths were dissected and stored in immersion oil on a glass slide for ~3 d to "clear" prior to reading. Prepared otoliths were read along the longest axis at 400x magnification using a Zeiss Axio compound microscope fit with a QImaging camera and Image Pro Premier 9.1 software. Larval otoliths were visible through the top of the cranium prior to dissection and growth increments were well defined. Otolith microstructure revealed three distinct growth regions after a prominent hatch-check: (1) fast growth and wide increments for ~3–7 d, (2) consistently slow growth and narrow increments for about 12 d, followed by (3) increasing growth increments to the otolith's edge (Supplementary Figure S2). Each otolith was read twice by the same reader without access to any sampling data. If the two reads differed by ≤5%, one read was randomly chosen for analysis. If reads differed by >5%, the otolith was read a third time. Otoliths where the three reads differed by >5% were removed from analysis ($n = 1$; Sponaugle *et al.*, 2010).

We enumerated daily increments to provide an estimate of age and used two metrics to analyze growth patterns: (1) mean daily growth (MDG) which is the average increment width of each day of life and (2) mean recent growth (MRG), which is the average increment widths of each individual over the last three full days of life (Supplementary Figure S2). We used the latter to best align with sampled environmental conditions because it is unknown how long larvae had been associated with the environmental conditions (including prey and predators) at the time of collection.

Because otolith increment width increases with the age of the fish, we detrended the last three increment widths for age by calculating a detrended growth index:

$$DG_{ij} = \left(G_{ij} - G_j\right) SD_j^{-1}, \quad (1)$$

where DG_{ij} is the detrended growth of individual i at age j, G_{ij} is otolith-based growth (increment width) for individual i at age j, G_j is the mean otolith-based growth of all individuals at age j, and SD is the standard deviation of G. Detrending growth of the last three full days of life (i.e. last three complete increment widths) for age allows us to compare the MRG of differently aged larvae (Robert *et al.*, 2009; Sponaugle *et al.*, 2010).

We compared MRG across cruises and locations using analysis of covariance (ANCOVA) with age as a covariate. There were no significant interactions between age and cruise or location prohibiting the interpretation of ANCOVA results. ANCOVAs were followed by a Tukey HSD post-hoc test, when applicable.

Diet analysis

We examined the gut contents of all larval northern lampfish used in otolith analysis that had intact guts ($n = 174$). Most larvae collected during winter 2018 storm conditions had damaged guts, hence W18 fish were excluded from diet analysis.

Larval guts were dissected in a few drops of glycerol on a microscope slide under a Leica MZ16 dissecting scope. We removed the entire gastrointestinal tract and then gently teased out prey using minutien pins, starting with the anterior end (Llopiz and Cowen, 2008). Prey were identified to the lowest taxonomic level possible, enumerated, and measured along the longest dimension (prosome length, carapace length, or total length) under the Leica MZ16 dissecting microscope with a QImaging camera and Image Pro Premier 9.1 software. Prey lengths were converted to biomass with published length to dry weight conversions, using temperate system conversions whenever possible (Uye, 1982; Berggreen *et al.*, 1988; Webber and Roff, 1995; Lindley *et al.*, 1999; Kaeriyama and Tsutomu, 2002; Cornet-Barthaux *et al.*, 2007; Nakamura *et al.*, 2017). When copepod order could not be discerned, we used the conversion provided for the pooled copepod community ("total copepodia"; Uye, 1982). Unknown crustacean biomass was estimated with the mean of the conversions used for all crustacean prey groups.

We calculated feeding incidence as the percentage of larval northern lampfish with prey in their gut. Larvae with no prey in their gut were excluded from all other diet analyses ($n = 38$). Three metrics were used to describe larval diet composition: frequency of occurrence (%FO; % of larvae with a particular prey type in the gut), numerical percentage (%N; % of each prey type out of all prey types consumed), and relative biomass (%B; % biomass of each prey type out of total consumed prey biomass). These metrics were calculated for every prey type in each season and location. Because larvae had a broader size range in summer (5.3–12.0 mm SL) compared to winter (5.1–7.9 mm SL), summer larvae were split into small (<8 mm SL) and large (>8 mm SL) size classes to investigate differences in feeding incidence and diet composition across season considering potential ontogenetic changes in feeding habits.

Consumed prey biomass was calculated for each larva by summing the dry weights of all consumed prey. We divided this value by larval SL^3 to account for increased gut capacity with larval size. These calculations were also performed for each individual prey group. Finally, we calculated standardized gut fullness as the residuals of the linear relationship between consumed prey biomass and larval SL^3 (Dower *et al.*, 1998). We use SL^3 instead of SL, which is traditionally used (Gleiber *et al.*, 2020), because post-flexion growth in northern lampfish entails a substantial increase in body depth (more so than length). Mean standardized consumed prey biomass and gut fullness were compared across seasons and locations using Wilcoxon rank sum tests (non-parametric) and Welch's t-tests (parametric), respectively. T-tests were used to compare gut fullness because one group (NH winter) had a parametric distribution and t-tests are robust to non-normality as long as sample size is large (n = ~30). There was no significant difference in total standardized consumed prey biomass or gut fullness between years ($p = 0.12$ and $p = 0.22$, respectively) or size classes ($p = 0.42$ and $p = 0.13$, respectively) in summer so these groups were pooled.

Prey availability and potential predation pressure

ISIIS imagery data were processed following Luo *et al.* (2018) and Schmid *et al.* (2020), with the full pipeline code open-sourced in Schmid *et al.* (2021). After automated classification, images were probability filtered following Failletaz *et al.* (2016), achieving 90% predictive accuracy per taxon. A random subsample of images was then classified by a human annotator and the results compared with the automated classification. The resulting confusion matrix was used to correct taxa concentrations during post-processing [Correction factor(taxon) = Precision(taxon)/Recall(taxon)]. Corrected taxa concentration estimates and co-collected physical data were kriged onto a grid equal to the length of each transect at 2-m vertical and 500-m horizontal resolution.

Prey groups of interest were selected based on our gut content analysis. We focused our analysis on prey taxa that varied substantially in their importance to larval diets across seasons and/or locations: calanoid copepods, copepod nauplii, and protists. While copepod nauplii are an important prey resource for northern lampfish (see the "Results" section), they are not quantitatively captured by ISIIS due to their small size and indistinct morphology. Thus, biological ring-net samples were used to supplement imagery data to capture the copepod nauplii group. Since all prey groups were standardized to concentration, the nauplii data could be easily integrated for a more holistic evaluation of prey availability.

There is a paucity of data on predation upon larval fishes in the NCC to inform potential predator selection. Predation by zooplankton is rarely quantified because of the variety of potential predators (Bailey and Houde, 1989) and the difficulty in sampling some taxa (i.e. gelatinous taxa) with net-based systems. Yet, several studies indicate that larval fishes may make up a significant portion of the diets of some taxa including chaetognaths, ctenophores, siphonophores, and hydromedusae (reviewed in Alvarino, 1985; Purcell, 1985). Anecdotally, northern lampfish have been observed in the gastric cavities of ctenophores (Auth and Brodeur, 2006) and chaetognaths (the present study) in the NCC, so these taxa were selected as the potential predator groups for analysis.

Mean prey and potential predator concentrations (ind. m^{-3}) were calculated for shelf and offshore portions of each transect (delineated by the shelf break, 200-m isobath). For the imagery data, mean taxa concentration was computed for each 1-m vertical bin down to 50-m depth. For the ring-net data, mean taxa concentration was computed for all net tows on the shelf and off the shelf along each transect.

Statistical modelling

We used generalized additive models (GAMs) to examine the effect of upwelling, prey availability, and potential predation pressure on the recent larval growth of northern lampfish. The response variable in this model was the individual MRG (last three full days) of 174 northern lampfish, which was the subset of larvae used in growth analysis with intact guts. The covariates were upwelling (continuous), *in situ* temperature (continuous), and protist (continuous, log transformed), copepod nauplii (continuous, log transformed), calanoid copepod (continuous, log transformed), and predator (continuous, log transformed) concentrations. We also incorporated an early growth parameter (mean increment width over the first third of each fish's life), as an individual's recent growth is likely impacted by their growth history (i.e. fish that grow fast early in life are more likely to continue growing fast later in life; Pepin *et al.*, 2015). Finally, we tested the use of a random effect (intercept) of net tow to account for the fact that individuals from the same MOCNESS tow are more likely to have similar growth, but model selection indicated that models without the random intercept were best.

Upwelling was the cumulative daily Coastal Upwelling Transport Index (CUTI; https://mjacox.com/upwelling-indices/) 10 d prior to capture. This period was selected to account for the lag between physical forcing and phyto- and zooplankton abundance. It is thought that phyto- and zooplankton lag wind stress by ~7 and ~13–16 d, respectively (Spitz and Allen, 2005). Because CUTI is a measure of vertical transport following wind stress, we chose the intermediate lag of 10 d. Temperature was calculated from MOCNESS environmental data, as the mean per net associated with each fish collection. We included temperature in the model to examine the role of upwelling after considering the well-documented effect of temperature on metabolically induced growth (Gillooly *et al.*, 2001). This is important to account for in upwelling systems where temperature and production often have an inverse relationship. Mean concentrations of protists (imagery data), copepod nauplii (ring-net data), calanoid copepods (imagery data), and predators (ctenophores and chaetognaths combined; imagery data) used corresponded to the location of fish collection on each transect. Predator taxa were pooled due to collinearity.

Variance inflation factors (VIF) indicated that correlations between covariates were not problematic (values ≤ 3; Zuur *et al.*, 2010). Smoothing functions were applied to each covariate and the number of knots was restricted to four to avoid model overfitting. A backward stepwise approach for model selection was used to compare full and reduced versions of the models and the model with the lowest Akaike's information criterion (AIC) and generalized cross validation (GCV) was chosen as the best model if it was the simpler version. If the model with the lowest AIC and GCV was the more complex model, it was only selected if it differed significantly (ANOVA, $p < 0.05$) from the reduced version. Model residuals were checked for deviations from normality, homogeneity of variance, and other abnormalities. All modelling analyses were conducted using the R software (v 4.0.4) package "mgcv" (Wood, 2021).

Results

Environmental setting

Upwelling varied seasonally and latitudinally throughout the sampling. In general, and consistent with expectations, upwelling was stronger in summer compared to winter and in northern California (TR) relative to Oregon (NH). Cumulative upwelling 10 d prior to sampling ranged from 0.81 to 21.02 m^3s^{-1} (Table 1). The mean cumulative upwelling was lowest during W19 in both locations. Off Oregon (NH), the strongest upwelling 10 d prior to sampling occurred during S19, while northern California (TR) experienced the most intense upwelling during S18, which was more than 3x greater than the following summer (S18 = 19.59 m^3s^{-1}, S19 = 6.20 m^3s^{-1}). Both locations experienced interannual variability in

Table 1. Northern lampfish (*S. leucopsarus*) concentration, upwelling during sampling, and concentrations of environmental prey (protists, copepod nauplii, and calanoid copepods) and predators (chaetognaths and ctenophores) sampled along the NH and TR Lines during the winters and summers of 2018 and 2019.

	Winter			Summer		
	All	NH	TR	All	NH	TR
Northern lampfish (ind. 1000 m^{-3})	17.1 (±4.7)	15.3 (±4.3)	19.1 (±8.6)	34.0 (±4.5)	21.0 (±6.3)	46.0 (±6.2)
Upwelling (CUTI; m^3s^{-1})	4.1 (0.8–12.9)	2.5 (0.8–4.3)	6.3 (2.9–12.9)	8.2 (3.0–21.0)	3.4 (3.0–3.9)	12.9 (5.5–21.0)
Prey						
Protists (ind. m^{-3})1	9.8 (±1.6)	12.7 (±2.1)	6.9 (±2.0)	21.1 (±3.2)	17.8 (±6.5)	23.5 (±3.2)
Copepod nauplii (ind. m^{-3})	3754.7 (±644.5)	4146.3 (±1298.0)	3363.1 (±488.6)	6995.2 (±1088.6)	6673.8 (±1742.0)	7316.5 (±1462.3)
Calanoid copepods (ind. m^{-3})	29.0 (± 16.7)	17.1 (± 3.7)	40.9 (± 31.8)	44.0 (± 9.2)	70.8 (± 15.5)	23.9 (± 3.7)
Predators						
Chaetognaths, ctenophores (ind. m^{-3})	2.9 (±0.5)	4.4 (±0.5)	1.3 (±0.3)	3.4 (±0.5)	2.9 (±0.7)	3.7 (±0.8)

Column "All" summarizes the mean winter and summer taxa concentration across both locations and years. Northern lampfish were sampled with a MOCNESS, copepod nauplii with a ring net, and all other taxa with the *In situ* Ichthyoplankton Imaging System (ISIIS). Upwelling values are the cumulative daily CUTI (Coastal Upwelling Transport Index; https://mjacox.com/upwelling-indices/) 10 d prior to each sampling event. Concentrations are reported as mean ± SE and upwelling is mean and range. Data are separated by year in Supplementary Table S1.

upwelling within each season, but the magnitude of variability was much greater in TR relative to NH (Figure 2).

Kriged temperature profiles aligned well with expectations based on the upwelling experienced during each sampling event. The water column was well mixed throughout winter sampling, but vertical thermal stratification existed during summer sampling with the thermocline shoaling toward the shelf in NH and TR both years. Vertical stratification was especially strong at NH where surface waters (<10-m) were up to ∼5–9°C warmer than those at depth (∼50-m). The summer water column was moderately more well mixed at TR. Summer surface temperatures were fairly uniform across the TR shelf, while NH exhibited cooler inshore and warmer offshore surface waters beyond the upwelling front (Supplementary Figure S3).

Northern lampfish distribution

Northern lampfish were the most abundant larval fish throughout our sampling ($n = 6563$), accounting for 13.7% of the total abundance of larval fishes in the winter and 32.3% in the summer. The overall mean concentration of larval northern lampfish was 27.7 (± 3.3) ind. 1000 m^{-3} and ranged from 2.2 (± 1.3; W18) to 55.0 (± 8.7; S18) ind. 1000 m^{-3} across cruises (Supplementary Table S1). Concentrations were generally higher in summer than in winter and at TR relative to NH (Table 1). Larvae were broadly distributed across the shelf throughout our sampling effort (Figure 1). They were concentrated in the upper 75-m of the water column, declining in abundance to 100-m. Larvae used in analysis were caught at a mean temperature of 10.6°C in the winter and 10.7°C in the summer.

Northern lampfish size, age, and growth

Larvae subject to growth analysis ranged in size from 5.0 to 12.0 mm SL and were 2–55 d post hatch (dph). Though the largest (>9 mm SL, >1.75 mm body depth) and oldest (>45 dph) larvae were only present in the summer, there was general coherence in size and age across seasons (Figure 3). Less than 6% of larvae were ≥ 40 dph. The overall population somatic growth rate was 0.11 mm d^{-1}. There was a significant positive relationship between fish size vs. age, otolith size vs. age, and the fish size-at-age residuals vs. otoliths size-at-age residuals in all years, seasons, and locations except for W18 TR, due to low sample size ($n = 6$; Supplementary Table S2).

MRG (mean growth over the last three full days of life) was significantly slower in winter than in summer during both years at NH ($p < 0.001$) and in 2019 at TR ($p < 0.001$; Figure 4). The non-significant difference in MRG between 2018 seasons at TR ($p = 0.39$) is likely due to small sample size (W18, $n = 6$). There was no significant within-season interannual variability in MRG, except for TR summer, when MRG was significantly faster in S19 than in S18 ($p = 0.001$; Figure 4B). Finally, there was no significant difference in MRG between locations during any cruise ($p = 0.26$, $p = 0.72$, $p = 0.67$, and p = 0.41 for W18, S18, W19, and S19, respectively).

Similarly, MDG (mean increment widths for each day of life) and size-at-age (otolith radius-at-age) varied by season; in both years, fish grew faster, and attained larger sizes-at-age in summer than in winter (Figure 5). This variability was apparent at all ages. At ∼15 dph, larvae at TR were growing significantly faster and were larger-at-age in S19 relative to S18 (Figure 5B and D). Winter interannual differences could not be examined at TR due to low sample size. At NH within season interannual variability in MDG and size-at-age was minimal (Figure 5A and C).

Northern lampfish diet

Northern lampfish feeding incidence was ∼20.9% higher in summer than in winter. Feeding incidence was similar across locations in both seasons, differing by no more than 5.2% between NH and TR (Table 2). Similarly, standardized consumed prey biomass, gut fullness, and diet composition varied across cruises with diet differences greater between seasons than among locations.

Larval northern lampfish consumed more prey and had fuller guts in summer compared to winter, with significantly higher standardized ingested prey biomass (NH $p = 0.04$, TR $p < 0.001$) and gut fullness (NH $p = 0.04$, TR $p = 0.003$) in both locations (Figure 6). There was no significant difference in standardized ingested prey biomass or gut fullness between years ($p = 0.12$ and $p = 0.22$, respectively) or summer larval fish size classes ($p = 0.42$ and $p = 0.13$, respectively).

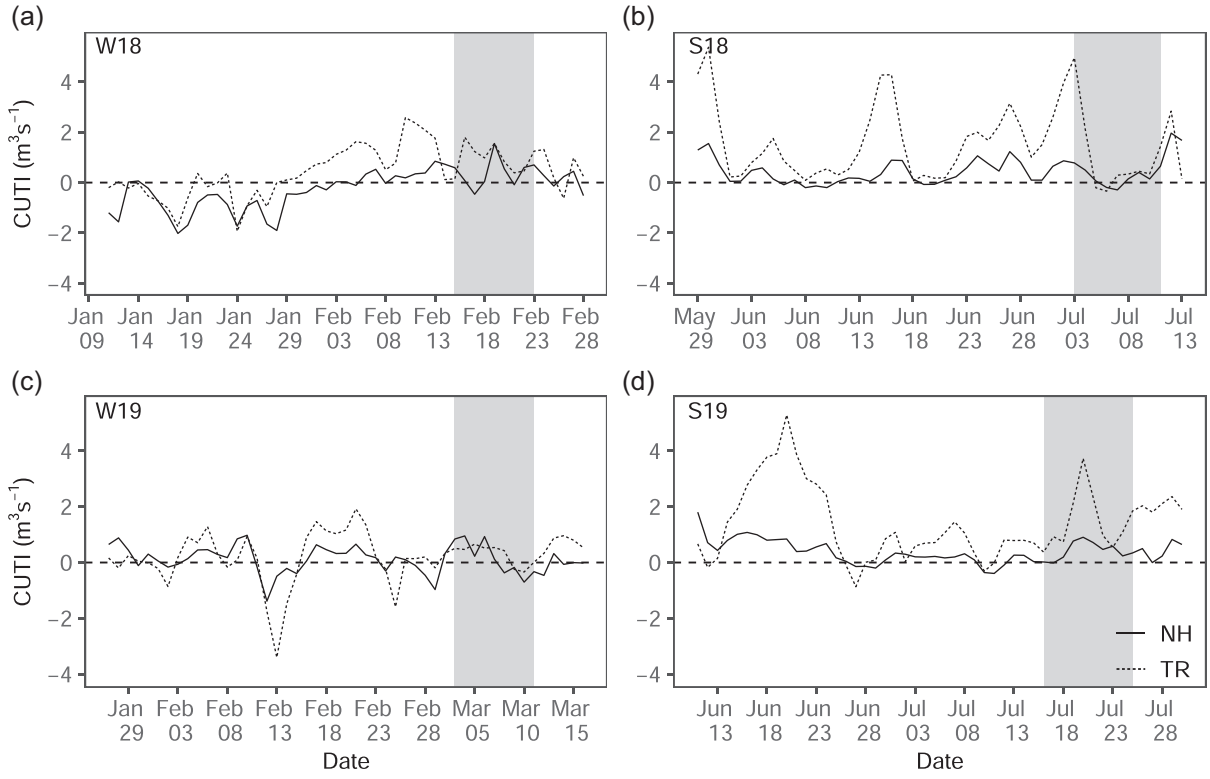

Figure 2. Daily CUTI for the NH (45°N; solid line) and the TR Lines (41°N; dotted line) during (a) winter 2018 (W18), (b) summer 2018 (S18), (c) winter 2019 (W19), and (d) summer 2019 (S19), with sampling dates highlighted in grey. Positive values signify upwelling, zero are neutral conditions, and negative values are downwelling.

In winter, northern lampfish larvae primarily consumed euphausiid calyptopsis (46.3%) and copepod nauplii (45.0%), which comprised >90% of their total ingested biomass. In summer, while larvae continued to consume these taxa, they also incorporated calanoid copepods into their diets. Calanoid copepods (26.1%) were the second largest contributor to summer total ingested biomass and were important for both larger (>8 mm SL; 41.3%) and smaller (<8 mm SL; 7.5%) larvae (Figure 7B). However, the size of ingested calanoid copepods differed between summer size classes, with larger larvae consuming significantly larger calanoid copepods (0.58 ± 0.03 mm prosome length) than smaller larvae (0.45 ± 0.04 mm prosome length; $p = 0.01$). Ostracods were regularly ingested throughout the year, and protists were consumed only in winter, as reflected in ingested prey counts (Figure 7A).

Larvae ingested a significantly higher biomass of copepod nauplii and protists in both locations in winter (NH $p = 0.002$, TR $p < 0.001$ and NH $p = 0.03$, TR $p = 0.02$, respectively) and calanoid copepods in summer (NH $p = 0.03$, TR $p = 0.01$; Figure 8A and B). Interannual differences in ingested biomass were only apparent in TR, where larvae consumed a substantially higher biomass of calanoid copepods in S19 compared to S18 and a moderately higher biomass of ostracods in S18 compared to S19 (Figure 8C and D).

Prey availability and potential predation pressure

Prey availability differed more between seasons than locations, with the concentration of protists and calanoid copepods roughly 1.5–2x higher in summer than in winter ($p = 0.02$ and $p = 0.002$, respectively). There was no significant difference in copepod nauplii abundance between summer and winter ($p = 0.08$), as they attained high concentrations throughout our sampling effort (Table 1). This seasonal pattern largely held within each location, except for calanoid copepods at TR in 2018 ($p = 0.90$) and protists at NH ($p = 0.94$). The typical seasonal pattern of higher summer calanoid abundance was evident at TR in 2019 ($p = 0.03$; Supplementary Table S1). Predation pressure also varied seasonally, but only at TR, where predators (chaetognaths and ctenophores) were more abundant in summer ($p = 0.03$; Table 1). Within each season, there was no significant locational difference in protist or copepod nauplii concentration (winter $p = 0.09$, summer $p = 0.48$; winter $p = 0.66$, summer $p = 0.58$, respectively), but calanoid copepods were significantly more abundant at NH than TR in summer ($p = 0.008$). The same was true for predators in winter ($p = 0.008$; Table 1). Finally, there were no significant within-season interannual differences in protist, copepod nauplii, and calanoid copepod availability in either location, but predators were more abundant in S19 than in S18 at TR ($p = 0.03$; Supplementary Table S1).

Recent growth modelling

The MRG of northern lampfish was influenced by environmental conditions, prey availability, and potential predation pressure (Figure 9; deviance explained = 48.6%). MRG displayed a dome-shaped relationship with upwelling intensity

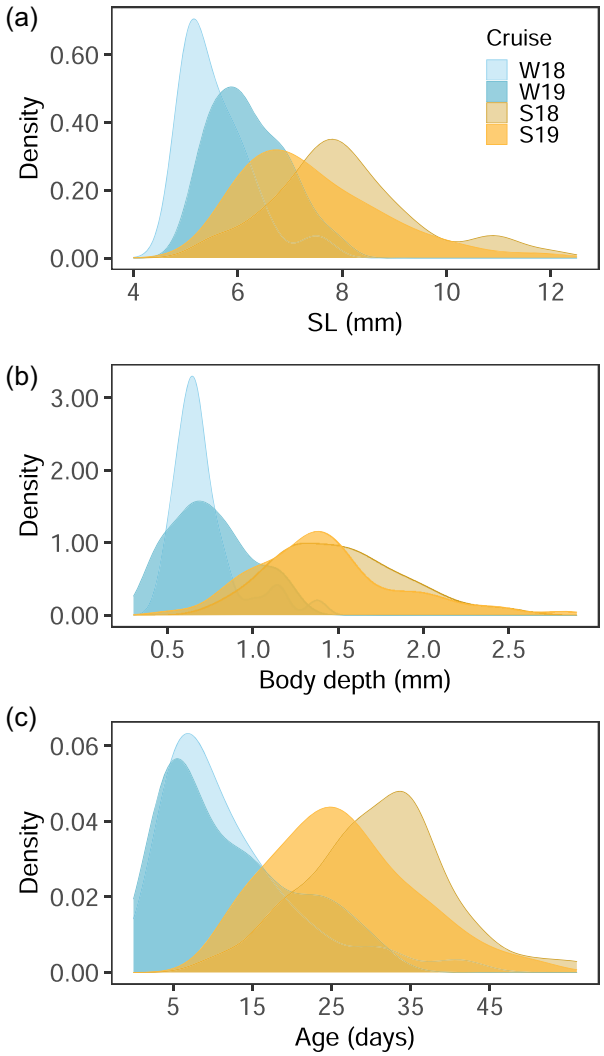

Figure 3. (a) Size (SL), (b) body depth, and (c) age frequency distributions of northern lampfish (*S. leucopsarus*) examined for otolith and gut content analysis. Fish were sampled from the NCC during the winters (blues) and summers (golds) of 2018 and 2019. W18 = winter 2018, W19 = winter 2019, S18 = summer 2018, S19 = summer 2019

($p < 0.001$): growth was lower than average during the weakest upwelling and rapidly increased to a peak at intermediate values before decreasing, but largely remaining above average, at the most intense upwelling experienced in TR during S18 (Figure 9A). However, we note that interpretation of predicted MRG at intermediate upwelling values is challenged by low sample size. MRG was strongly and positively affected by temperature ($p < 0.001$), with above-average growth at temperatures > 11°C (Figure 9B). When environmental calanoid copepod concentrations were low, northern lampfish larvae had below average MRG, whereas they had above average MRG at high calanoid copepod concentrations ($p = 0.002$; Figure 9D). The opposite was true for copepod nauplii concentrations, which had a weaker and negative impact on MRG ($p = 0.009$; Figure 9C). Finally, northern lampfish growth was consistently below average at increasing predator concentrations but increased quickly at the highest predator concentrations experienced throughout sampling ($p = 0.005$; Figure 9E).

Discussion

Northern lampfish larvae exhibited significant differences in growth and diet across NCC upwelling regimes, with greater seasonal than latitudinal variability. Growth was generally faster in the summer, when upwelling was stronger and larvae consumed more calanoid copepods, fewer copepod nauplii and protists, and had substantially higher gut fullness, than in the winter. During reduced upwelling in the winter, slower-growing larvae had guts that were less full and diets that were dominated by lower-trophic-level prey (i.e. protists and copepod nauplii). These patterns resulted in summer larvae that were significantly larger-at-age than winter larvae. However, when summer upwelling was the most intense, and despite comparable environmental prey availability, larval northern lampfish consumed fewer calanoid copepods, grew more slowly, and were smaller-at-age than in more moderate upwelling conditions. Finally, high zooplanktivorous predation pressure was correlated to above average growth, which may indicate a selective loss of slower-growing larvae that are less able to escape predation (Anderson, 1988; Gleiber *et al.*, 2020).

Larval northern lampfish otolith microstructure

Larval northern lampfish grew at a somatic growth rate of 0.11 mm d^{-1}, which is comparable to other slower-growing, high-latitude myctophids (Methot, 1981; Moku *et al.*, 2001). Their otoliths were comprised of well-defined bands with three distinct growth regions after a prominent hatch-check: (1) fast growth and wide bands for approximately 3–7 d, (2) consistently slow growth and thin bands for about 12 d, followed by (3) increasing growth increments to the otolith's edge. Nishimura et al. (figure 4B, 1999) also observed this growth pattern on the interior section of adult northern lampfish otoliths and a similar growth history is evident in another larval myctophid in the region, *Tarletonbeania crenularis* (figure 3 in Bystydzieńska *et al.*, 2010). Interestingly, despite having very similar morphology and growth rates (0.13 mm d^{-1}), the growth pattern of larval *D. theta* is quite different, with increments gradually increasing in width from the core to the otolith edge (figure 1A in Moku *et al.*, 2001). The discrepancy in larval growth patterns between northern lampfish and *D. theta* may provide a mechanism to confidently discern between morphologically similar species.

Seasonal variability in larval northern lampfish diet and growth

Similar to other larval myctophids, the diet composition of northern lampfish consisted of protists, ostracods, larval euphausiids, copepod nauplii, and cyclopoid and calanoid copepods (Conley and Hopkins, 2004; Sassa and Kawaguchi, 2005). However, larval diets were affected by seasonal variability in the plankton community. Of particular importance is the environmental abundance of copepod nauplii and calanoid copepods relative to their seasonal importance in northern lampfish diets. During reduced upwelling in winter, northern lampfish primarily consumed copepod nauplii. They continued to feed on nauplii in summer upwelling conditions, but also incorporated calanoid copepods into their diets. This resulted in northern lampfish with a substantially greater relative biomass of nauplii in their guts in winter compared to summer. Yet, copepod nauplii were equally available in the environment in both seasons. In contrast, when the availability

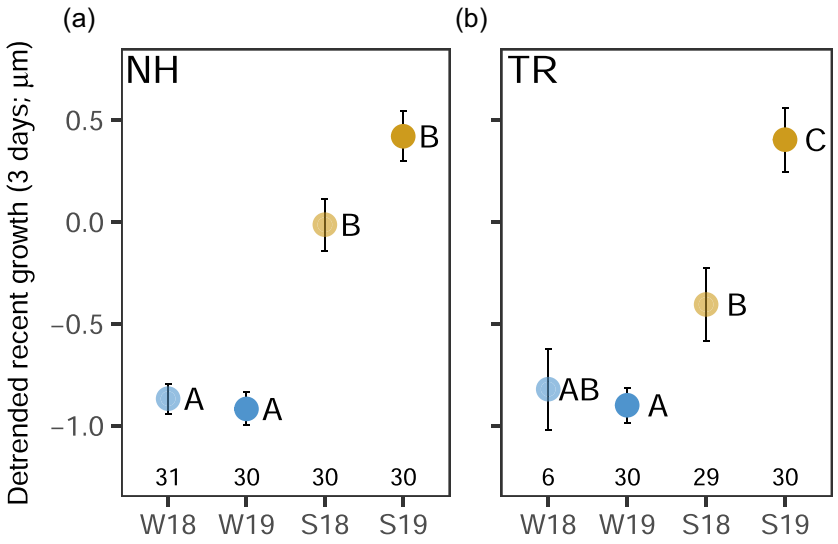

Figure 4. Mean ± SE detrended growth during the last three complete days of life (MRG) of northern lampfish (*S. leucopsarus*) collected in the winter (blues) and summer (golds) of 2018 and 2019 along the (a) NH and the (b) TR Lines. Significance is indicated to the right of each data point, with points sharing letters not significantly different from each other ($p \geq 0.05$). Sample sizes are indicated above the x-axis. W18 = winter 2018, W19 = winter 2019, S18 = summer 2018, and S19 = summer 2019

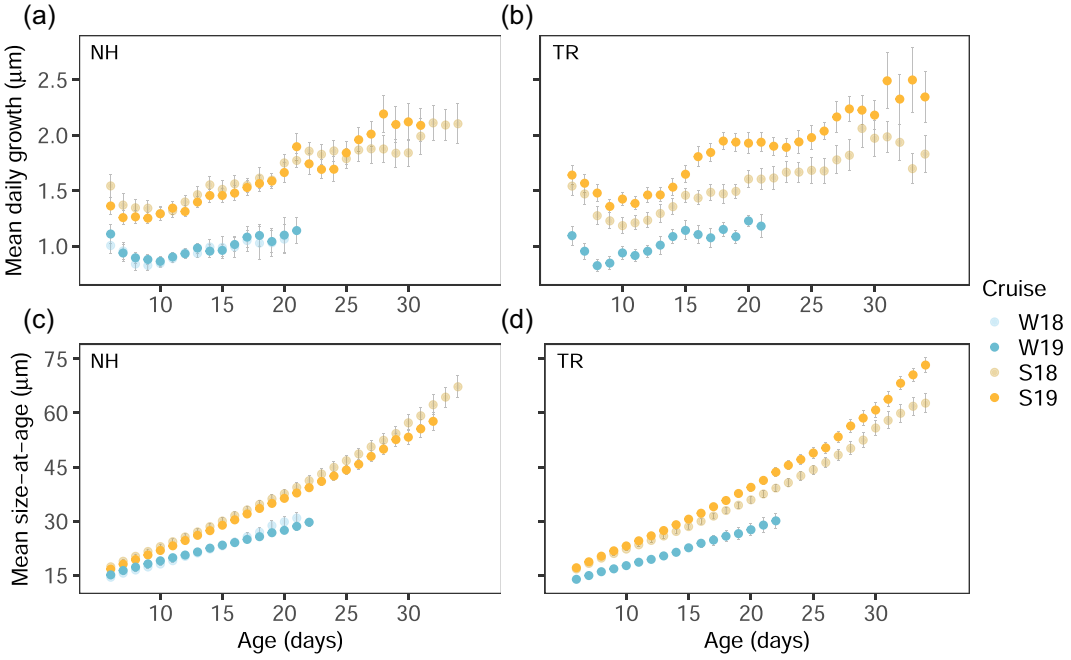

Figure 5. Mean ± SE (a, b) daily growth (otolith increment width) and (c, d) size-at-age (otolith radius-at-age) of larval northern lampfish (*S. leucopsarus*) collected in the NCC in winter (blues) and summer (golds) of 2018 and 2019 on the (a, c) NH and the (b, d) TR Lines. Ages were truncated when $n < 5$ observations. W18 = winter 2018, W19 = winter 2019, S18 = summer 2018, and S19 = summer 2019

of calanoid copepods increased in summer, their biomass in larval northern lampfish diets significantly increased. These patterns suggest that larval northern lampfish respond opportunistically to increases in calanoid copepods. Although larger northern lampfish consumed more calanoid copepods, preferential feeding on calanoids cannot be attributed to an ontogenetic shift in diet, as this pattern holds for winter and summer larvae in the same size class (5–8 mm SL). Preference for calanoid copepods has been observed for multiple species of larval fish in a variety of systems including, among others, larval tunas (*Thunnus atlanticus*) in the Straits of Florida (Gleiber *et al.*, 2020), Atlantic cod (*Gadus morhua*) in the Gulf of St. Lawrence (Robert *et al.*, 2011), and European hake (*Merluccius merluccius*) in the Catalan Sea (Morote *et al.*, 2011). Further evidence for dietary selection is evident in larval consumption of the lowest trophic level prey (i.e. protists). Protist ingestion was restricted to the less productive winter season, even though they were twice as abundant in summer.

Our findings indicate that northern lampfish larvae can respond to the more productive food-web during enhanced

Table 2. Summary of diet data for larval northern lampfish (*S. leucopsarus*) collected in the NCC in the winter of 2019 and summers of 2018 and 2019 along the NH and the TR Lines.

	Winter						Summer (<8 mm SL)						Summer (>8 mm SL)					
	All		NH		TR		All		NH		TR		All		NH		TR	
Larvae, *n* =	58		28		30		75		38		37		41		20		21	
Prey, *n* =	146		78		68		190		107		83		159		81		78	
Fish size (mm SL)	5.1–7.9		5.1–7.9		5.2–7.6		5.3–8.0		5.5–7.9		5.3–8.0		8.1–12.0		8.1–12.0		8.2–11.8	
Feeding incidence (%)	65.5		67.9		63.3		80.0		78.9		81.1		92.7		90		95.2	
Prey type	%N	%FO	%N	%FO	%N	%FO	%N	%FO	%N	%FO	%N	%FO	%N	%FO	%N	%FO	%N	%FO
Copepoda																		
Calanoida	0.0	0.0	0.0	0.0	0.0	0.0	5.8	14.2	2.8	7.5	9.6	22.9	23.3	57.9	24.7	53.1	21.8	62.8
Cyclopoida	0.7	2.7	1.3	5.1	0.0	0.0	2.1	6.3	3.7	11.2	0.0	0.0	4.4	25.2	4.9	37.0	3.8	12.8
Unknown	0.7	2.7	1.3	5.1	0.0	0.0	1.6	7.9	0.9	1.9	2.4	15.7	1.3	11.9	1.2	8.6	1.3	15.4
Nauplius	70.5	87.7	62.8	84.6	79.4	91.2	38.4	69.5	45.8	75.7	28.9	61.4	34.6	68.6	30.9	64.2	38.5	73.1
Euphausiacea																		
Calyptopis	8.9	24.7	11.5	34.6	5.9	13.2	26.8	61.1	27.1	62.6	26.5	59.0	13.8	46.5	11.1	48.1	16.7	44.9
Ostracoda																		
Ostracoda	11.0	37.7	15.4	47.4	5.9	26.5	15.8	42.6	10.3	39.3	22.9	47.0	15.7	50.3	19.8	54.3	11.5	46.2
Protists	6.8	9.6	5.1	7.7	8.8	11.8	0.0	0.0	0.0	0.0	0.0	0.0	0.0	0.0	0.0	0.0	0.0	0.0
Unknown crustacean	1.4	4.1	2.6	7.7	0.0	0.0	8.4	30.0	7.5	30.8	9.6	28.9	6.9	35.2	7.4	54.3	6.4	15.4
Unknown	0.0	0.0	0.0	0.0	0.0	0.0	1.1	2.1	1.9	3.7	0.0	0.0	0.0	0.0	0.0	0.0	0.0	0.0

Column "All" summarizes the mean winter and summer diet data across both locations and years. Feeding incidence is the percentage of larvae that consumed at least one prey item, and the diet is described with both numerical percentages of prey types (%N) and the frequencies of occurrence of prey types (%FO), defined as the percentage of feeding larvae with the prey type present. Summer data are split by size class.

summer upwelling by selectively feeding on higher-trophic-level prey (i.e. calanoid copepods). Heightened copepod abundance in summer is well documented in this seasonal system (Peterson and Miller, 1977). In addition to seasonal variability in overall copepod abundance, the copepod community also shifts between seasons. The winter downwelling community is typically dominated by warm-water copepods that are transported poleward in the Davidson Current, while the summer upwelling community is characterized by cold-water species transported to the NCC from subarctic source waters (Peterson and Miller, 1977; Hooff and Peterson, 2006). These subarctic copepods tend to accumulate lipids, making them an important prey base for many predator taxa (Peterson and Schwing, 2003; Hooff and Peterson, 2006; Tomaro *et al.*, 2012; Peterson *et al.*, 2014). While the adult forms of these species are likely too large (>3 mm prosome length) to be consumed by fish larvae in this study (5–12 mm SL), their smaller, younger, but still lipid-rich, life stages may provide superior nutrition for larval northern lampfish in summer (Peterson, 1986; Liu and Hopcroft, 2007).

Consumption of calanoids appears to be beneficial for northern lampfish growth and survival. A high reliance on nauplii biomass in winter resulted in reduced growth and smaller-at-age larvae, while less dependence on nauplii and the incorporation of calanoid copepods in summer led to faster growing and larger-at-age larvae. In seasonally productive systems, some prey taxa (i.e. copepod nauplii) are likely important for sustenance year-round, while other high value taxa (i.e. calanoid copepods) confer enhanced growth when available during more productive conditions (i.e. summer upwelling). Because northern lampfish have a protracted spawning season that places larvae in the pelagic water column during both optimal (summer) and suboptimal (winter) feeding environments, there are likely effects on larval survivorship as well as possible carry-over effects on growth and survival later in life.

It should be noted that although all sampling occurred during full daylight hours, daylength, photoperiod, and the intensity of solar input differs between winter and summer in the NCC. These metrics have the potential to impact the strength and magnitude of zoo- and ichthyoplankton vertical migrations, which may affect winter and summer comparisons of taxa concentrations in the upper water column. Some studies suggest that vertical migration distance decreases with increasing photoperiod (Conroy *et al.*, 2020), while others have found that migration amplitude is greater in the summer than the winter (Li *et al.*, 2021). It is thus difficult to discern the true impacts of seasonal differences in zoo- and ichthyoplankton vertical migrations on our results, not only due to these conflicting findings but also because most studies on this topic occurred in regions that experience more substantial changes to seasonal daylength (i.e. polar regions) than the NCC.

Interannual variability in larval northern lampfish diet and growth

Modelling individual recent growth across NCC upwelling regimes revealed a dome-shaped relationship, with growth peaking at intermediate upwelling intensities. Recent growth was below average when upwelling was minimal, but rapidly increased with moderate upwelling conditions. Growth then decreased again at the highest upwelling intensity (as measured in 2018 at TR). During that time, upwelling 10 d prior

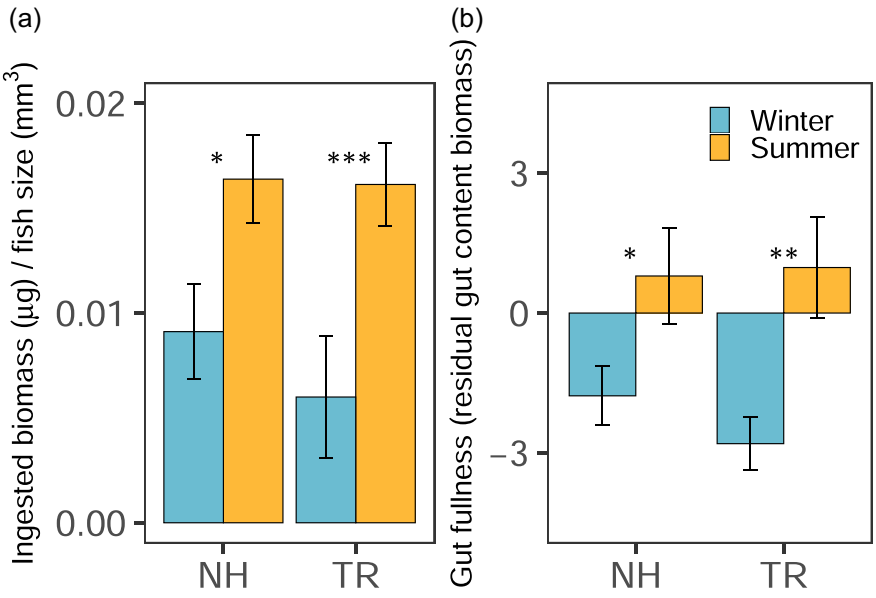

Figure 6. *Stenobrachius leucopsarus* (a) mean standardized total consumed prey biomass [µg dry weight/*S. leucopsarus* SL (mm^3)] and (b) mean gut fullness expressed as residual gut content biomass (residuals of total consumed prey biomass vs. SL^3) of larvae collected on the NH and the TR Lines during the winter (blue) and summer (gold) of 2018 and 2019. $^{***}p < 0.001$, $^{**}p < 0.01$, and $^{*}p < 0.05$

to sampling was 3x greater than the following year. Despite interannual variability in summer upwelling intensity at this location, ambient calanoid copepod abundances remained relatively consistent. Yet, fish consumed an order of magnitude lower calanoid copepod biomass resulting in significantly slower larval growth than they did the following year. Together, these findings suggest that there is a physical mechanism limiting feeding.

Theoretical models suggest larval fish feeding is not only determined by ambient food availability but also by larvae-prey encounter rates. Upwelling is typically accompanied by turbulent mixing of the nutrient-rich upper water column. When intense, upwelling-induced turbulence can negatively impact encounter rates between larval fishes and their prey, thereby reducing feeding success (Cury and Roy, 1989; MacKenzie *et al.*, 1994). The negative effects of too much upwelling-induced turbulence have been demonstrated for other species in the California Current. A common pleuronectid in the region (English sole, *Parophrys vetulus*) feeds most successfully in lower upwelling conditions when their preferred prey, appendicularians, are aggregated rather than dispersed (Alldredge, 1982; Gadomski and Boehlert, 1984). Similarly, too much upwelling-induced turbulence is thought to disrupt planktonic food aggregations for northern anchovy *(E. mordax*; Lasker, 1978, 1981). While empirical evidence for subsequent effects on recruitment to the adult population remain equivocal (Peterman and Bradford, 1987; Peterman *et al.*, 1988) and responses to upwelling related turbulence appear to be system, scale, and taxon (both predator and prey) dependent, our findings are consistent with the conceptional model that at low upwelling intensity, feeding is production limited while at high upwelling intensity it is turbulence limited.

Early life history success in seasonally driven systems

The NCC supports major fisheries of species whose larval and juvenile stages depend on upwelling-driven primary and secondary production. Yet, most NCC fishes spawn in winter when downwelling or reduced upwelling prevails and some species, such as northern lampfish, have protracted spawning seasons that encompass both winter (downwelling) and summer (upwelling) conditions (Richardson and Pearcy, 1977; Auth and Brodeur, 2006).

We found that northern lampfish consumed fewer and lower-trophic-level prey in the winter than in the summer, with significant effects on growth. This begs the question: what is the benefit of winter spawning? One possibility is that the need for larval retention nearshore outweighs the need for fast growth. Because nutrient supply is linked to offshore transport in upwelling systems, fishes must find a balance between transport/retention, feeding, and growth during their vulnerable early life history stages. A hypothesized solution to this problem is that fishes evolve reproductive strategies that place larvae in the pelagic realm during periods or locations that minimize the probability of offshore advection (Parrish *et al.*, 1981) while providing enough production for sustenance and slower, but sufficient, growth for survival.

Another possibility is that winter-spawned northern lampfish obtain a survival advantage later in life. In this system, the biological spring transition (typically April–May) follows the onset of upwelling and marks the arrival of a copepod community that is dominated by large, cold-water, lipid-rich species (see above; Hooff and Peterson, 2006). The presence of this highly nutritious prey base is vital for the feeding and survival of the early life history stages of NCC fishes (Peterson and Schwing, 2003; Hooff and Peterson, 2006; Tomaro *et al.*, 2012; Peterson *et al.*, 2014). However, these studies largely focused on the juvenile stage when fish can theoretically consume adult cold-water copepods with a prosome length of ~3 mm (Peterson, 1986; Liu and Hopcroft, 2007). Most marine fishes, including larvae, are gape-limited: larvae are initially constrained to small prey, with size of prey available to them increasing as they grow, especially for mid-to-high latitude taxa (Pepin and Penney, 1997; Llopiz, 2013). At the

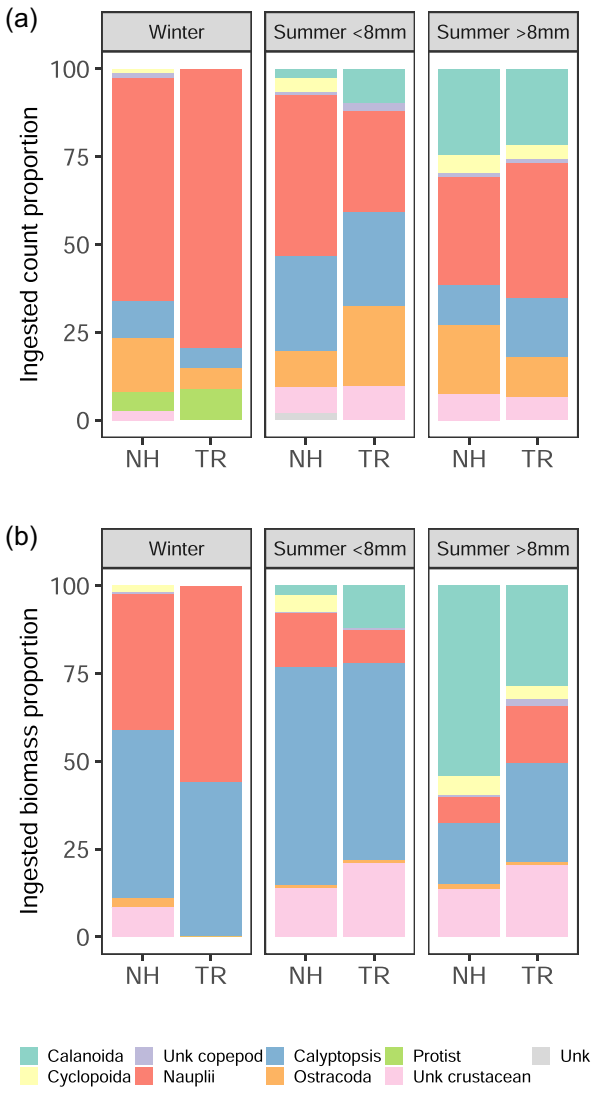

Figure 7. *Stenobrachius leucopsarus* larvae ingested prey (a) count and (b) biomass [μg dry weight], presented as proportion of all consumed prey collected along the NH and the TR Lines. Summer fish are separated into small (<8 mm SL) and large (>8 mm SL) categories to account for seasonal size differences. $n = 58$ (winter), $n = 75$ (summer < 8 mm), and $n = 41$ (summer >8 mm). Unk = unknown

biological spring transition, surviving winter-spawned larvae would be several months old, and although slower-growing, might be large enough to capitalize on the largest (adult) lipid-rich prey base typical of summer.

We found a significant ontogenetic shift in ingested calanoid copepod prey size, with larger larvae consuming larger calanoid copepods. Back-calculated birthdates indicate that at the biological spring transition (29 May, 2018 and 5 June, 2019), surviving winter-spawned northern lampfish would have been 3.5–4.5 months old (13 January–17 February birthdates) in 2018 and 3-4 months old (3 February–7 March) in 2019. While the larval duration for this species is unknown, an abrupt change in adult northern lampfish otolith microstructure at ~70 dph (Nishimura *et al.*, 1999) may indicate metamorphosis. Additionally, a similar species in the region is estimated to be 71 dph at juvenile transformation (*D. theta*, Moku *et al.*, 2001), thus winter-spawned northern lampfish are likely to be at or near transition to the juvenile stage at the time of the spring transition. Therefore, while winter-spawned northern lampfish have substantially lower feeding success and consequently slower larval growth than summer-spawned fish, winter-spawning may lead to a survival advantage for the juvenile stage in summer coinciding with availability of large, nutritious adult copepod prey. Such a tradeoff between fast and slow larval growth and subsequent juvenile success may underlie the persistence of a protracted spawning behaviour in seasonally driven systems. How this tradeoff carries over to successful recruitment to the adult population is unclear but likely varies among years.

Predation

Predator (chaetognath and ctenophore) abundances significantly influenced measured northern lampfish larval growth. After factoring in prey availability and environmental conditions, the partial effect of predators indicates that larval growth was consistently below average at low-to-mid range predator abundances and was above average at the highest concentration of predators. The finding of faster larval growth in high predator environments may be the result of predators selectively consuming smaller, slower-growing larvae (Gleiber *et al.*, 2020). While the abundance of these potential predators in our study only varied seasonally at TR, other multi-year studies have documented higher chaetognath and ctenophore abundances at NH in summer compared to winter (Peterson and Miller, 1976; Keister and Peterson, 2003). Further, other potential gelatinous predators, such as hydromedusae, can increase in abundance during upwelling conditions (Miglietta *et al.*, 2008). Such increased predator abundances may lead to enhanced summer predation pressure on northern lampfish. The "growth-mortality" hypothesis and its three corollaries ("bigger-is-better," "stage duration," and "growth-selective predation"), suggest that larger size, faster growth, and quicker development reduces vulnerability to predation (Anderson, 1988). Thus, fast larval growth may be important to the survival of summer-spawned larvae in the high-predator environment typical of summer. Although predation pressure will also be higher for winter-spawned northern lampfish at this time, they may be better suited to escape predation due their older age, larger size, and advanced developmental stage when they encounter the high-predator summer environment.

Mode of predation likely impacts the larval growth response. While we focused on the effects of gelatinous taxa, which tend to be passive (ctenophores, hydromedusae) or ambush (chaetognath) predators, active predators (e.g. some non-gelatinous zooplankton, higher trophic taxa) probably also predate upon larval northern lampfish, and the predator effect on growth likely differs between more passive and more active taxa. Predators that actively search out prey may selectively feed on larger prey items, which would result in a growth pattern opposite of that observed in our data (i.e. slower growth at high predation pressure due to the selective consumption of larger, faster-growing individuals).

In situ imagery allowed us evaluate predator distributions that could offset the perceived advantages of heightened feeding under certain upwelling regimes. Traditional net-based sampling techniques have limited our ability to resolve zooplanktivorous predation on larval fishes, especially for fragile gelatinous taxa. Nonetheless, predation may be the primary agent of larval mortality (Bailey and Houde, 1989) and

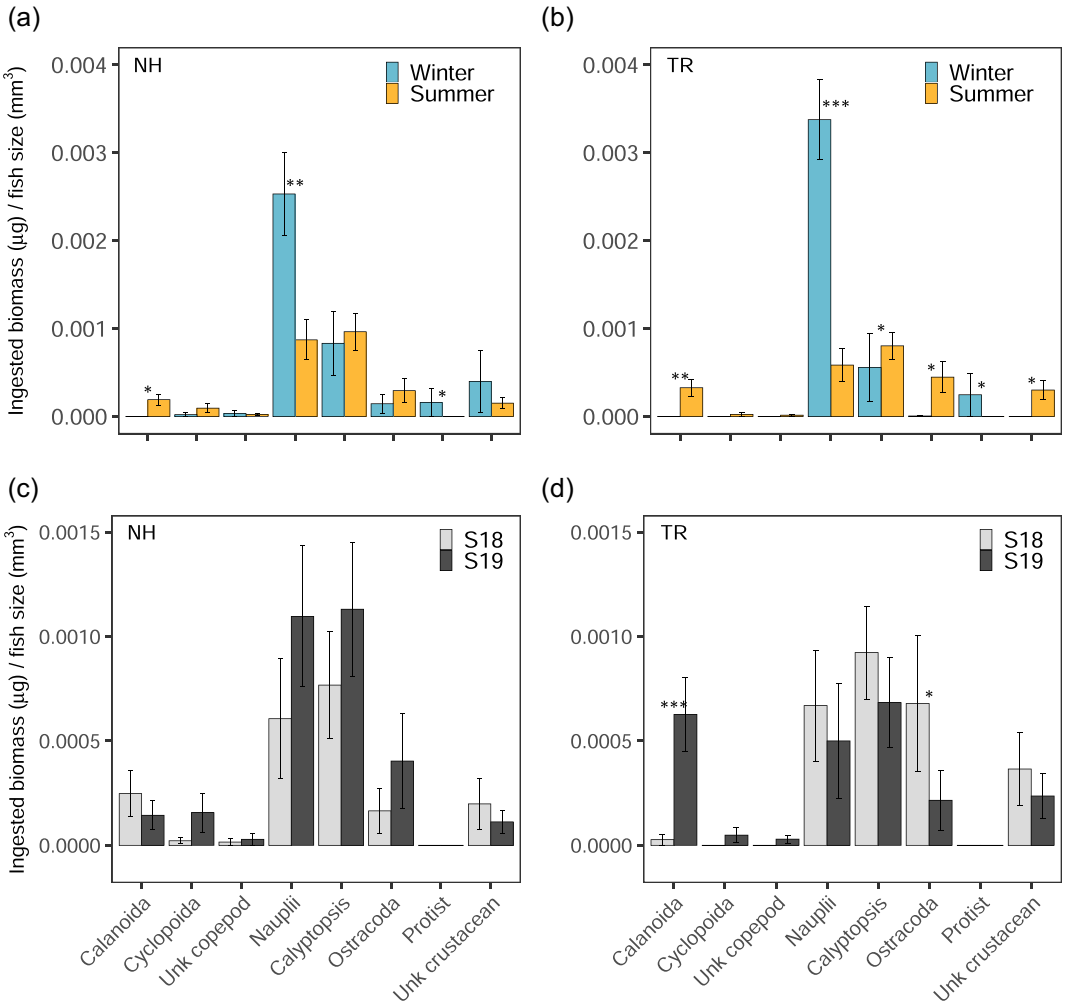

Figure 8. Seasonal (a, b) and interannual (c, d) northern lampfish (*S. leucopsarus*) mean standardized total consumed prey biomass [µg dry weight/*S. leucopsarus* SL (mm^3)] of individual prey groups on the (a, c) NH and the (b, d) TR Lines. S18 = summer 2018, S19 = summer 2019. $^{***}p < 0.001$, $^{**}p < 0.01$, and $^{*}p < 0.05$

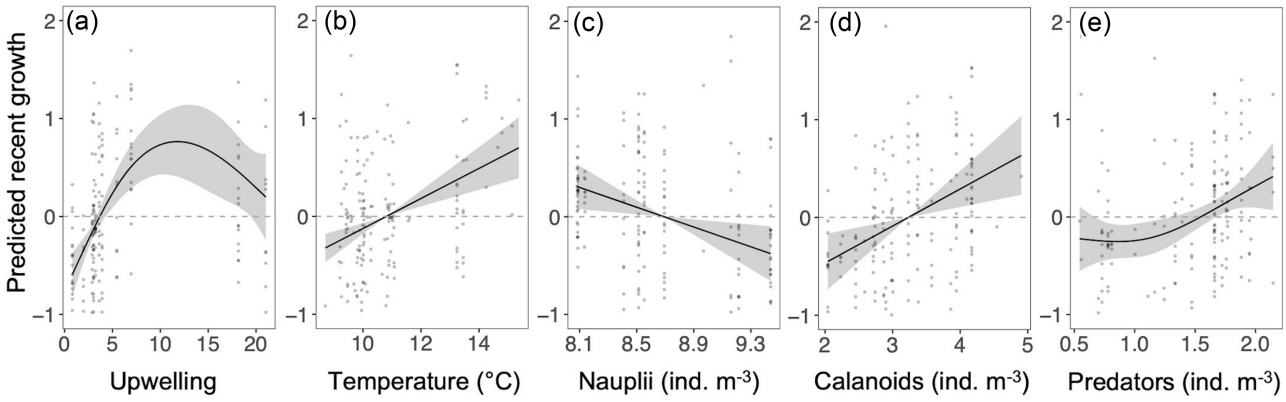

Figure 9. GAM smooth functions showing the partial effects of each covariate after accounting for the other covariate effects on the MRG (last 3 complete days) of individual larval northern lampfish (*S. leucopsarus*; $n = 174$). Upwelling is the cumulative CUTI ($m^3 s^{-1}$) 10 d prior to each fish collection and taxa concentrations are all log + 1 transformed. 95% confidence intervals (grey shading) and partial residuals (points) are shown for each covariate. Model AIC = 362.8, deviance explained = 48.6%

understanding the implications of variable predation pressure across upwelling regimes is necessary for a comprehensive examination of the influence of upwelling on larval survival. This need is greater than ever, as the abundance of some potential gelatinous predators is increasing in the NCC (Brodeur *et al.*, 2019).

Conclusions

In the NCC, most fishes spawn during winter downwelling or reduced upwelling and some have protracted spawning that encompasses multiple seasons. For the latter, understanding the growth and feeding repercussions of spawning phenology is important to elucidate the mechanisms underlying recruitment variability. Our findings demonstrate variability in larval northern lampfish feeding and growth across upwelling regimes, with moderate upwelling conditions conferring the fastest growth. While we suggest that winter-spawned larvae with slower larval growth may experience enhanced juvenile success once upwelling commences, this is likely to vary across years and extension of this work across life history stages is needed to tease apart these relationships. Finally, as interest in harvesting mesopelagic resources grows (Hidalgo and Browman, 2019), it is imperative that we understand the basic tenants of myctophid early life histories, including their growth and diets, and the relationship between these metrics and variable oceanographic conditions. Their role in the pelagic foodweb of such productive systems is understudied yet likely to be highly important.

Acknowledgements

We are grateful for the captains and crews of the R/V Sikuliaq, R/V Atlantis, and R/V Sally Ride for their contributions to at-sea sampling. We are especially indebted to H.W. Fennie, M. Wilson, K. Axler, M. Gleiber, and C. Briseño-Avena for their dedication to this study, which included spending up to 40 d at sea. This project was greatly improved through input on larval fish identification by T. Auth as well as modelling guidance from L. Ciannelli. Finally, we thank Oregon State University's Center for Quantitative Life Sciences, especially C. Sullivan, and the army of undergraduate volunteers at Oregon State University who contributed to the processing of imagery and plankton samples: D. Daprano, L. Nepstad, A. Branka, A. Bolm, C. Watson, B. Anders, A. Pulscak, L. Wetchler, J. Knowlton, N. Baker, R. Hartley, K. Bowditch, K. Rorvig, H. Woodwick, K. Bauer, Z. Sallada, S. Knodel, M. Sandmeier, H. Woodruff, Z. Thomas, and B. Rothman.

Supplementary data

Supplementary material is available at the *ICESJMS* online version of the manuscript.

Conflict of interest

None declared

Funding

This study was funded by the National Science Foundation Division of Ocean Sciences (NSF OCE-1737399). All samples were collected under Oregon State University ACUP permit 4960. KS was also supported through the Hatfield Marine Science Center Markham Award, the Walter G. Jones Fishery Development Award, the Hannah-Jones Award, and Integrative Biology Research Funds. During the preparation of this manuscript, S.S., R.K.C., M.S.S., and J.I. were supported by the National Science Foundation Division of Ocean Sciences grant NSF OCE-2125407, and K.R.S. was supported by NSF OCE-2125408.

Author contributions

KS conducted all laboratory analyses, data analysis, and manuscript preparation; SS served as co-PI, advised KS, and edited manuscript drafts; RKC, SS, and KRS designed larger study and obtained project funding; RKC was PI and chief scientist during all field work; MSS processed underwater imagery; JI processed and identified plankton samples; MCU sorted ring net samples; KS, RKC, MSS, JI, MCU, and KRS participated in field work.

Data availability

Most of the data underlying this article are available in the Biological and Chemical Oceanography Data Management Office (BCO-DMO) at https://www.bco-dmo.org/project/743417. Additional data are available upon request to the corresponding author.

References

Alldredge, A. L. 1982. Aggregation of spawning appendicularians in surface windrows. Bulletin of Marine Science, 32: 250–254.

Alvarino, A. 1985. Predation in the plankton realm; mainly with reference to fish larvae. Investigaciones marinas CICIMAR, 2: 1–122.

Anderson, J. T. 1988. A review of size dependent survival during prerecruit stages of fishes in relation to recruitment. Journal of Northwest Atlantic Fishery Science, 8: 55–66.

Auth, T. D., and Brodeur, R. D. 2006. Distribution and community structure of ichthyoplankton off the coast of Oregon, USA, in 2000 and 2002. Marine Ecology Progress Series, 319: 199–213.

Auth, T. D. 2008. Distribution and community structure of ichthyoplankton from the northern and central California Current in May 2004-06. Fisheries Oceanography, 17: 316–331.

Bailey, K., and Houde, E. 1989. Predation on eggs and larvae of marine fishes and the recruitment problem. Advances in Marine Biology, 25: 1–83.

Bakun, A. 2006. Fronts and eddies as key structures in the habitat of marine fish larvae: opportunity, adaptive response and competitive advantage. Scientia Marina, 70: 105–122.

Beamish, R. J., Leask, K. D., Ivanov, O. A., Balanov, A. A., Orlov, A. M., and Sinclair, B. 1999. The ecology, distribution, and abundance of midwater fishes of the Subarctic Pacific gyres. Progress in Oceanography, 43: 399–442.

Berggreen, U., Hansen, B., and Kiorboe, T. 1988. Food size spectra, ingestion and growth of the copepod *acartia tonsa* during development: implications for determination of copepod prodcution. Marine Biology, 99: 341–352.

Bograd, S. J., Schroeder, I., Sarkar, N., Qiu, X., Sydeman, W. J., and Schwing, F. B. 2009. Phenology of coastal upwelling in the California Current. Geophysical Research Letters, 36: 1–5.

Brodeur, R. D., and Yamamura, O. 2005. Micronekton of the North Pacific. PICES Scientific Report No, 30: 1–107.

Brodeur, R. D., Auth, T. D., and Phillips, A. 2019. Major shifts in pelagic micronekton and macrozooplankton community structure in an upwelling ecosystem related to an unprecedented marine heatwave. Frontiers in Marine Science, 6: 212.

Bystydzieńska, Z. E., Phillips, A. J., and Linkowski, T. B. 2010. Larval stage duration, age and growth of blue lanternfish *tarletonbeania crenularis* (Jordan and Gilbert, 1880) derived from otolith microstructure. Environmental Biology of Fishes, 89: 493–503.

Checkley, D. M., and Barth, J. A. 2009. Patterns and processes in the California Current System. Progress in Oceanography, 83: 49–64.

Conley, W. J., and Hopkins, T. L. 2004. Feeding ecology of lanternfish (Pisces: myctophidae) larvae: prey preferences as a reflection of morphology. Bulletin of Marine Science, 75: 361–379.

Conroy, J. A., Steinberg, D. K., Thibodeau, P. S., and Schofield, O. 2020. Zooplankton diel vertical migration during antarctic summer. Deep Sea Research Part I: Oceanographic Research Papers, 162: 103324.

Cornet-Barthaux, V., Armand, L., and Quéguiner, B. 2007. Biovolume and biomass estimates of key diatoms in the Southern Ocean. Aquatic Microbial Ecology, 48: 295–308.

Cowen, R. K., and Guigand, C. M. 2008. *In situ* ichthyoplankton imaging system (ISIIS): system design and preliminary results. Limnology and Oceanography: Methods, 6: 126–132.

Cury, P., and Roy, C. 1989. Optimal environmental window and pelagic fish recruitment success in upwelling areas. Canadian Journal of Fisheries and Aquatic Sciences, 46: 670–680.

Dower, J. F., Pepin, P., and Leggett, W. C. 1998. Enhanced gut fullness and an apparent shift in size selectivity by radiated shanny (*Ulvaria subbifurcata*) larvae in response to increased turbulence. Canadian Journal of Fisheries and Aquatic Sciences, 55: 128–142.

Failletta, R., Picheral, M., Luo, J. Y., Guigand, C., Cowen, R. K., and Irisson, J. 2016. Imperfect automatic image classification successfully describes plankton distribution patterns. Methods in Oceanography. 15-16: 60–77.

Fast, T. N. 1960. Some Aspects of the Natural History of Stenobrachius leucopsarus Eigenmann and Eigenmann. PhD Dissertation, Stanford University. Stanford, CA. 1–104.

Gadomski, D. M., and Boehlert, G. W. 1984. Feeding ecology of pelagic larvae of English sole *parophrys vetulus* and butter sole *isopsetta isolepis* off the Oregon coast. Marine Ecology Progress Series, 20: 1–12.

García-Reyes, M., and Largier, J. 2012. Seasonality of coastal upwelling off central and northern California: new insights, including temporal and spatial variability. Journal of Geophysical Research: Oceans, 117: C03028.

Gillooly, J., Brown, J., West, G., Savage, V., and Charnov, E. 2001. Effects of size and temperature on metabolic rate. Science, 293: 2248–2251.

Gleiber, M. R., Sponaugle, S., and Cowen, R. K. 2020. Some like it hot, hungry tunas do not! implications of temperature and plankton food web dynamics on growth and diet of tropical tuna larvae. ICES Journal of Marine Science, 77: 3058–3073.

Guigand, C. M., Cowen, R. K., Llopiz, J. K., and Richardson, D. E. 2005. A coupled asymmetrical multiple opening closing net with environmental sampling system. Marine Technology Society Journal, 39: 22–24.

Hare, J. A., and Cowen, R. K. 1997. Size, growth, development, and survival of the planktonic larvae of *Pomatomus saltatrix* (Pisces: pomatomidae). Ecology, 78: 2415–2431.

Hidalgo, M., and Browman, H. I. 2019. Developing the knowledge base needed to sustainably manage mesopelagic resources. ICES Journal of Marine Science, 76: 609–615

Hooff, R. C., and Peterson, W. T. 2006. Copepod biodiversity as an indicator of changes in ocean and climate conditions of the northern California current ecosystem. Limnology and Oceanography, 51: 2607–2620.

Houde, E. D. 2008. Emerging from Hjort's shadow. Journal of Northwest Atlantic Fishery Science, 41: 53–70.

Kaeriyama, H., and Tsutomu, I. 2002. Body allometry and developmental characteristics of the three dominant pelagic ostracods (*Discoconchoecia pseudodiscophora*, *Orthoconchoecia haddoni* and *Metaconchoecia skogsbergi*) in the Oyashio region, western North Pacific. Plankton Biology and Ecology, 49: 97–100.

Keister, J. E., and Peterson, W. T. 2003. Zonal and seasonal variations in zooplankton community structure off the central Oregon coast, 1998–2000. Progress in Oceanography, 57: 341–361.

Lasker, R. 1978. The relation between oceanographic conditions, and larval anchovy food in the California Current: identification of factors contributing to recruitment failure. Rapports et proces-verbaux des Réunions. Conseil International pour l'Éxploration de la Mer, 173: 212–230.

Lasker, R. 1981. Factors contributing to variable recruitment of the nothern anchovy (*Engraulis mordax*) in the California Current: contrasting years 1975 through 1978. Rapports et proces-verbaux des Réunions. Conseil International pour l'Éxploration de la Mer, 178: 375–388.

Lindley, J., Robins, D., and Williams, R. 1999. Dry weight carbon and nitrogen content of some euphausiids from the north Atlantic Ocean and the Celtic Sea. Journal of Plankton Research, 21: 2053–2066.

Li, T., Liu, T., Liu, R., and Chen, L. 2021. Diel vertical migration of dominant panktonic crustaceans in the south branch of the Yangtze Estuary, China. Aquaculture and Fisheries, 6: 414–423.

Liu, H., and Hopcroft, R. R. 2007. A comparison of seasonal growth and development of the copepods *Calanus marshallae* and *C. pacificus* in the northern Gulf of Alaska. Journal of Plankton Research, 29: 569–581.

Llopiz, J. K., and Cowen, R. K. 2008. Precocious, selective and successful feeding of larval billfishes in the oceanic Straits of Florida. Marine Ecology Progress Series, 358: 231–244.

Llopiz, J. K. 2013. Latitudinal and taxonomic patterns in the feeding ecologies of fish larvae: a literature synthesis. Journal of Marine Systems, 109-110: 69–77.

Luo, J. Y., Irisson, J. - O., Graham, B., Guigand, C., Sarafraz, A., Mader, C., and Cowen, R. K. 2018. Automated plankton image analysis using convolutional neural networks. Limnology and Oceanography: Methods, 16: 814–827.

MacKenzie, B. R., Miller, T. J., Cyr, S., and Leggett, W. C. 1994. Evidence for a dome-shaped relationship between turbulence and larval fish ingestion rates. Limnology and Oceanography, 39: 1790–1799.

Matarese, A., Kendall Jr., A., Blood, D., and Vinter, B. 1989. Laboratory guide to early life history stages of northeast Pacific fishes. NOAA Technical Report NMFS, 80: 1–652.

McClatchie, S., Cowen, R., Nieto, K., Greer, A., Luo, J. Y., Guigand, C., Demer, D. *et al.* 2012. Resolution of fine biological structure including small narcomedusae across a front in the Southern California Bight. Journal of Geophysical Research: Oceans, 117: n/a–n/a.

McClatchie, S., Gao, J., Drenkard, E. J., Thompson, A. R., Watson, W., Ciannelli, L., Bograd, S. J., *et al.* 2018. Interannual and secular variability of larvae of mesopelagic and forage fishes in the southern California Current system. Journal of Geophysical Research: Oceans, 123: 6277–6295.

Methot, R. D. 1981. Spatial covariation of daily grow th rates of larval northern anchovy, *Engraulis mordax*, and larval northern lampfish, *Stenobrachius leucopsarus*. Rapports et proces-verbaux des Réunions. Conseil International pour l'Éxploration de la Mer, 178: 424–431.

Miglietta, M. P., Rossi, M., and Collin, R. 2008. Hydromedusa blooms and upwelling events in the Bay of Panama, Tropical East Pacific. Journal of Plankton Research, 30: 783–793.

Miller, T. J., Crowder, L. B., Rice, J. A., and Marschall, E. A. 1988. Larval size and recruitment mechanisms in fishes: toward a conceptual framework. Canadian Journal of Fisheries and Aquatic Sciences, 45: 1657–1670.

Moku, M., Ishimaru, K., and Kawaguchi, K. 2001. Growth of larval and juvenile *diaphus theta* (Pisces: myctophidae) in the transitional waters of the western North Pacific. Ichthyological Research, 48: 385–390.

Morote, E., Olivar, M. P., Bozzano, A., and Villate, F. 2011. Feeding selectivity in larvae of the European hake (*Merluccius merluccius*) in relation to ontogeny and visual capabilities. Marine Biology, 158: 1349–1361.

Nakamura, A., Matsuno, K., Abe, Y., Shimada, H., and Yamaguchi, A. 2017. Length-weight relationships and chemical composition of the dominant mesozooplankton taxa/species in the subarctic pacific, with special reference to the effect of lipid accumulation in copepoda. Zoological Studies, 56: 13.

Nishimura, A., Nagasawa, K., Asanuma, T., Aoki, H., and Kubota, T. 1999. Age, growth, and feeding habits of lanternfish, *stenobrachius leucopsarus* (myctophidae), collected from the near-surface layer in the Bering Sea. Fisheries Science, 65: 11–15.

Parrish, R. H., Nelson, C. S., and Bakun, A. 1981. Transport mechanisms and reproductive success of fishes in the California Current. Biological Oceanography, 1: 175–203.

Pepin, P., and Penney, R. 1997. Patterns of prey size and taxonomic composition in larval fish: are there general size-dependent models? Journal of Fish Biology, 51: 84–100.

Pepin, P., Robert, D., Bouchard, C., Dower, J. F., Falardeau, M., Fortier, L., Jenkins, G. P., *et al.* 2014. Once upon a larva: revisiting the relationship between feeding success and growth in fish larvae. ICES Journal of Marine Science, 72: 359–373.

Peterman, R., and Bradford, M. 1987. Wind speed and mortality rate of a marine fish, the northern anchovy (*Engraulis mordax*). Science, 235: 354–356.

Peterman, R. M., Bradford, M. I., Lo, N. C. H., and Methot, R. D. 1988. Contribution of early life stages to interannual recruitment of northern anchovy (*Engraulis mordax*). Canadian Journal of Fisheries and Aquatic Sciences, 45: 8–16.

Peterson, W. 1986. Development, growth, and survivorship of the copepod *Calanus marshallae* in the laboratory. Marine Ecology Progress Series, 29: 61–72.

Peterson, W., Fisher, J., Peterson, J., Morgan, C., Burke, B., and Fresh, K. 2014. Applied fisheries oceanography: ecosystem indicators of ocean conditions inform fisheries management in the California Current. Oceanography, 27: 80–89.

Peterson, W. T., and Miller, C. 1976. Zooplankton along the continential shelf off Newport, Oregon, 1969-1972: distribution, abundance, seasonal cycle, and year-to-year variations. Sea Grant Reports, 1–114.

Peterson, W. T., and Miller, C. B. 1977. Seasonal cycle of zooplankton abundance and species composition along the central Oregon coast. Fishery Bulletin, 75: 717–724.

Peterson, W. T., and Schwing, F. B. 2003. A new climate regime in northeast pacific ecosystems. Geophysical Research Letters, 30: OCE6.

Postel, L., Fock, H., and Hagen, W. 2000. Biomass and abundance. In Zooplankton Methodology Manual, ICES, pp. 83–192. Ed. by R. Harris, P. Wiebe, H. Skjoldal, and M. Huntdley. Academic Press, London.

Purcell, J. E. 1985. Predation on fish eggs and larvae by pelagic cnidarians and ctenophores. Bulletin of Marine Science, 37: 739–755.

Richardson, S. L., and Pearcy, W. G. 1977. Coastal and oceanic fish larvae in an area of upwelling off Yaquina Bay, Oregon. Fishery Bulletin, 75: 125–145.

Robert, D., Castonguay, M., and Fortier, L. 2009. Effects of preferred prey density and temperature on feeding success and recent growth in larval mackerel of the southern Gulf of St. Lawrence. Marine Ecology Progress Series, 377: 227–237.

Robert, D., Levesque, K., Gagné, J. A., and Fortier, L. 2011. Change in prey selectivity during the larval life of Atlantic cod in the southern Gulf of St Lawrence. Journal of Plankton Research, 33: 195–200.

Robert, D., Murphy, H., Jenkins, G., and Fortier, L. 2014. Poor taxonomical knowledge of larval fish prey preference is impeding our ability to assess the existence of a 'critical period' driving year-class strength. ICES Journal of Marine Science, 71: 2042–2052.

Sassa, C., and Kawaguchi, K. 2005. Larval feeding habits of Diaphus theta, *Protomyctophum thompsoni*, and *Tarletonbeania taylori* (Pisces: myctophidae) in the transition region of the western North Pacific. Marine Ecology Progress Series, 298: 261–276.

Schmid, M., Cowen, R., Robinson, K., Luo, J., Briseño-Avena, C., and Sponaugle, S. 2020. Prey and predator overlap at the edge of a mesoscale eddy: fine-scale, in-situ distributions to inform our understanding of oceanographic processes. Scientific Reports, 10: 921.

Schmid, M., Daprano, D., Jacobson, K. M., Sullivan, C., Briseño-Avena, C., Luo, J. Y., and Cowen, R. K. 2021. A convolutional Neural network based high-throughput image classification pipeline - code and documentation to process plankton underwater imagery using local HPC infrastructure and NSF's XSEDE. [Software] https://zenodo.org/record/4641158 (last accessed 12 January 2022).

Smoker, W., and Pearcy, W. G. 1970. Growth and reproduction of the lanternfish *Stenobrachius leucopsarus*. Journal of the Fisheries Research Board of Canada, 27: 1265–1275.

Spitz, Y., and Allen, J. 2005. Modeling of ecosystem processes on the Oregon shelf during the 2001 summer upwelling. Journal of Geophysical Research, 110: C10S17.

Sponaugle, S., Walter, K. D., Denit, K. L., Llopiz, J. K., and Cowen, R. K. 2010. Variation in pelagic larval growth of Atlantic billfishes: the role of prey composition and selective mortality. Marine Biology, 157: 839–849.

Takahashi, M., Checkley, D. M., Litz, M. N., Brodeur, R. D., and Peterson, W. T. 2012. Responses in growth rate of larval northern anchovy (*Engraulis mordax*) to anomalous upwelling in the northern California Current. Fisheries Oceanography, 21: 393–404.

Tomaro, L., Teel, D., Peterson, W., and Miller, J. 2012. When is bigger better? Early marine residence of middle and upper Columbia River spring Chinook salmon. Marine Ecology Progress Series, 452: 237–252.

Uye, S. 1982. Length-weight relationships of important zooplankton from the inland Sea of Japan. Journal of the Oceanographical Society of Japan, 38: 149–158.

Webber, M., and Roff, J. 1995. Annual biomass and production of the oceanic copepod community off Discovery Bay, Jamaica. Marine Biology, 123: 481–495.

Wood, S. 2021. mgcv. R package version 1.8-38. https://cran.r-project.org/web/packages/mgcv/mgcv.pdf (last accessed 12 January 2022).

Zuur, A. F., Leno, E. N., and Elphick, C. S. 2010. A protocol for data exploration to avoid common statistical problems. Methods in Ecology and Evolution, 1: 3–14.

Handling Editor: Szymon Smolinski